Orientation dependence of interface motion in ^{4}He crystals induced by acoustic waves

R. Nomura,* S. Kimura, F. Ogasawara, H. Abe, and Y. Okuda
Department of Condensed Matter Physics, Tokyo Institute of Technology, 2-12-1, O-okayama, Meguro-ku, Tokyo 152-8551, Japan
(Received 5 December 2003; revised manuscript received 13 April 2004; published 20 August 2004)

The interface motion of a ^{4}He crystal induced by an acoustic wave was investigated. When an acoustic wave was applied from the liquid side, it induced melting of the crystal. When applied from the crystal side, melting was induced at high temperatures and crystallization was induced at low temperatures [Nomura *et al.*, Phys. Rev. Lett. **90**, 075301 (2003)]. This means that the direction of the force on the interface was inverted at an inversion temperature T_i. The displacement induced by an acoustic wave pulse was systematically studied in crystals with different surface orientations and it was found that T_i decreased when approaching the *c* facet. The observed interface motion was analyzed by assuming that it was induced by the acoustic radiation pressure.

DOI: 10.1103/PhysRevB.70.054516 PACS number(s): 67.80.−s, 68.08.−p, 81.10.−h

I. INTRODUCTION

Ordinary crystal growth involves three main processes: transport of atoms to the interface, crystallization kinetics at the interface, and transport of the latent heat released by the crystallization. However, when a ^{4}He crystal grows in a superfluid at low temperature, the first and third processes are very fast and cannot be limiting processes in this system. This is a model system to study fundamental aspects of crystal growth and also anomalous interface phenomena, which are sometimes hidden by the bulk transport and difficult to investigate systematically in ordinary materials.[1–3] Examples of such phenomena are propagation of crystallization waves,[4–6] drastic enhancement of ultrasound reflection at the interface,[7–12] instability induced by a uniaxial stresse,[13,14] effect of heat flow on the interface,[15] effect of superfluid flow,[16,17] and so on.

Acoustic radiation pressure is a dynamical force which works at a surface where the acoustic impedance changes discontinuously.[18–20] It is a second order acoustic effect and can be calculated by averaging the force on the surface for a longer period than that of the acoustic wave. It is also possible to interpret it as a momentum transfer from phonons to the surface.[21] It has been widely used as a tool to manipulate an object without a direct contact, and was also used for investigating the dynamics of liquid drops and for passive stabilization of liquid capillary bridges at low-gravity.[22–24] However, it is not known whether acoustic radiation pressure can induce a first order phase transition and crystallization in a fluid. We have recently demonstrated that crystallization, melting and nucleation of ^{4}He crystal can be induced by acoustic waves at low temperatures.[25,26] We attributed this effect to the acoustic radiation pressure which induced the interface motions. When acoustic waves were applied to the crystal-liquid interface perpendicularly from the liquid side, it induced melting of the crystal at all experimental temperatures. Direction of the force was the same as the acoustic waves in this condition. However, when acoustic waves were applied to the crystal-liquid interface perpendicularly from the crystal side, the crystal was melted at high temperatures and was grown at low temperatures. This means that direction of the force on the interface was inverted at an inversion temperature T_i.[25] It was also reported that the interface was moved by an acoustic wave parallel to the interface: either melting or crystallization was stochastically induced in the vicinity of the transducer.[26]

We systematically measured anisotropy in the interface motion induced by longitudinal acoustic waves for crystals with different surface orientations. Acoustic waves were applied perpendicularly to the interface in this report. It was found that T_i was lower for a vicinal surface than for a rough surface, and decreased from 0.8 to 0.6 K when approaching the *c* facet. Temperature, acoustic wave power and pulse duration dependences were investigated and compared with an acoustic radiation pressure model. We had a reasonable agreement with the model in the low-temperature region. At high temperatures, the agreement was not good and another melting mechanism was needed to explain the observations.

II. EXPERIMENTS AND RESULTS

Experiments were performed in a cell that was cooled by a dilution refrigerator; the cell was the same one as used in a previous paper.[25] It had two optical windows for the crystal to be optically observable from room temperature through infrared filters and infrared absorption glasses. Temperature was measured by a RuO_2 thermometer in the cell and pressure by a capacitive pressure gauge. Two transducers of the longitudinal mode, which were made of $LiNbO_3$ with coaxial electrodes, were placed in the cell about 10 mm apart. Effective diameters of the transducers were about 5 mm and their resonance frequency was about 10 MHz. The diameters were much larger than the wavelength of the acoustic wave. We can regard the acoustic wave as a plane wave under this condition. Acoustic waves were directed in the vertical direction. When we grew a large ^{4}He crystal in the cell, it filled the lower space of the cell. The position of the crystal-liquid interface was adjusted so that it was midway between the transducers by observing the height of the crystal. Images were recorded by a normal video camera or a high-speed camera. Gravity caused the interface to be flat on a horizontal plane. Acoustic waves were applied perpendicular to the

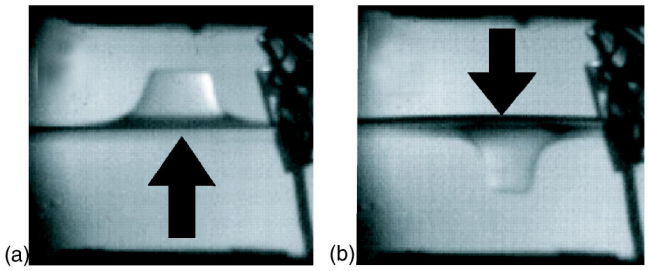

FIG. 1. Crystallization and melting induced by acoustic waves for a vicinal surface at low temperatures. Arrows in the figure indicate the direction of the acoustic waves. Crystal-liquid interface moved in the same direction as the acoustic waves although the direction was inverted at higher temperatures in an acoustic wave from the crystal side.

interface. Acoustic waves were applied upward or from the crystal side by the lower transducer and downward or from the liquid side by the upper transducer. The interface motions of a vicinal surface induced by continuous acoustic waves are shown in Fig. 1. An acoustic wave induced a swell on the interface or crystallization when it was applied to the vicinal surface from the crystal side [Fig. 1(a)] and induced a hollow or melting when applied from the liquid side [Fig. 1(b)]. A clear *c* facet appeared on the top of the swell and the bottom of the hollow in both cases on the vicinal surface, because anisotropies in surface stiffness and growth rate were very strong on the vicinal surface. As we have reported in Ref. 25, the shape of the swell and the hollow induced by the acoustic wave was rounded on a rough surface. Morphologies of the swell and the hollow on the vicinal surface were quite different from those on the rough surface.

Continuous acoustic waves induced large enough displacements for us to observe them with a video camera. However, we were unable to avoid heating which disturbed the system too much to make a systematic measurement of the temperature dependence of the interface motion. We, thus, adopted an acoustic wave pulse method in order to manipulate and detect the displacement of the interface. Displacement of the interface induced by the acoustic wave pulse of 1 msec duration was 200 μm or less and the interface relaxed to the equilibrium position within a few tens of msec after the pulse in the fastest case. Optical measurement of the displacement was not accurate and rapid so we adopted the acoustic wave to monitor the position of the interface during the relaxation. Time sequences of the acoustic pulses are schematically shown in the inset of Fig. 2. The interface was lifted (crystallized) or lowered (melted) by the manipulation pulse and then was relaxed to the equilibrium position by gravity. The motion of the interface was detected from the phases of the acoustic wave pulses transmitted through the interface making use of the sound velocity difference in the crystal and the liquid. Displacement of the interface h is related to the phase difference $\Delta\phi$ of the transmitted monitoring pulse as

$$\Delta\phi = \omega\left(\frac{1}{c_c} - \frac{1}{c_l}\right)h, \tag{1}$$

where ω is the angular frequency of the acoustic wave, c_c and c_l are sound velocity in the crystal and the liquid. Pulse

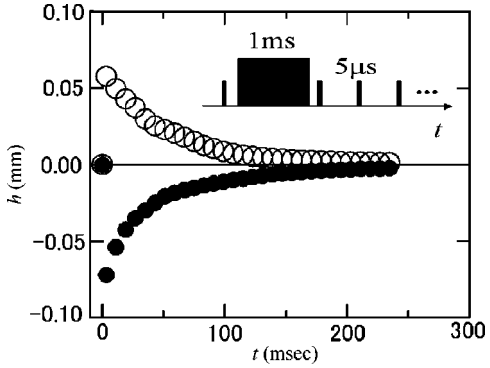

FIG. 2. Relaxation of surface height after the manipulation pulse at $T=725$ mK for a rough surface. Open circles are the case of the acoustic wave from the crystal side and closed circles are from the liquid side. The inset shows the time sequence of acoustic wave pulses.

interval of the monitoring pulses was changed from 5 to 100 msec depending on the time constant of the relaxation. Pulse duration of the monitoring pulses was 5 μsec and their power was reduced about −8 dB from the manipulation pulse. Effect of the monitoring pulse on the interface motion was neglected at this power, pulse duration, pulse interval and in our experimental temperature ranges. This method has made it possible to make faster and more accurate measurements than the video camera, though we can obtain only spatially averaged information on the interface. The manipulation pulse, which was applied from the crystal side or the liquid side by the same transducer, has a much longer duration of 1 msec. Effect of the reflected wave was neglected because the reflection signal was about 5 times smaller than the first transmitted signal. The displacement h induced by this manipulation pulse was the quantity we wanted to measure. We could obtain h from the displacement just after the manipulation pulse in the relaxation process. A typical time evolution of the displacement is shown in Fig. 2 for a rough surface at $T=725$ mK. The manipulation pulse was applied at $t=0$. Time constants of the relaxation agreed well with those calculated from the growth coefficients measured by Amrit *et al.* for various surface orientations.[12] Thus, we can say that the densities of the defects in our crystals were not high compared with the crystals used in other experiments.

In order to determine c_c we grew the crystal up to the upper transducer and filled the space between the two transducers. Surface orientation θ measured from the *c* axis was mostly determined from c_c using the elastic constant of hcp ^{4}He crystal measured by Crepeau *et al.*[27] except for C_{33}. For the crystals with $\theta < 10°$, it was also possible to determine θ visually during a sample growth process because a clear *c* facet appeared in the process. We measured $c_c = 549 \pm 2$ m/sec for a crystal with $\theta = 2 \pm 1°$ and obtained the elastic constant $C_{33} = 5.76 \times 10^7$ kg/s^{2}m with better accuracy than that of Crepeau *et al.* We used this C_{33} and others by Crepeau *et al.* to calculate θ. In the region $50° < \theta < 90°$, θ is a double value function of c_c and cannot be determined uniquely. However, most of the crystals we grew had $\theta < 50°$ and only one crystal had $\theta > 50°$.

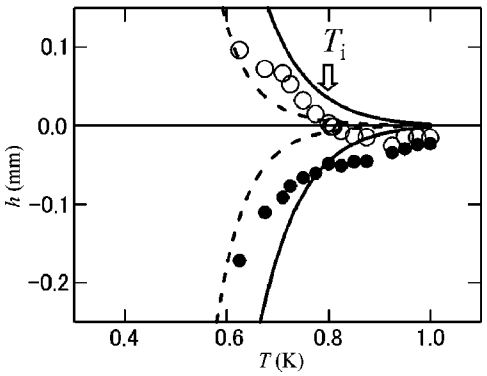

FIG. 3. Temperature dependence of the displacement induced by an acoustic wave pulse of 1 msec duration for a rough surface (crystal A, $\theta=43°$). Open (closed) circles are the case of the acoustic wave from the crystal (liquid) side. From the crystal side, crystallization was induced below T_i and melting above T_i. Lines are calculations from the acoustic radiation pressure model explained in the text.

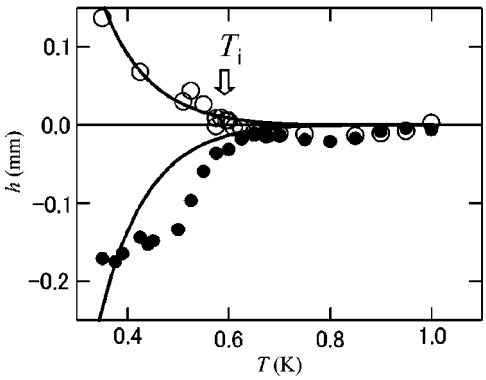

FIG. 4. Temperature dependence of the displacement induced by an acoustic wave pulse of 1 msec duration for a vicinal surface (crystal B, $\theta=2°$). Open (closed) circles are the case of the acoustic wave from the crystal (liquid) side. T_i was lower for the vicinal surface than for rough surfaces. Lines are calculations from the acoustic radiation pressure model explained in the text.

Power calibration of an acoustic wave was done by making use of a balance of the acoustic radiation pressure and the gravity at the gas-liquid interface. It was performed at low temperature where the damping of acoustic wave in the superfluid could be neglected. Acoustic radiation pressure is well known to induce a motion of an interface between two fluids. Gas-liquid interface of ^{4}He or a free surface of superfluid in this case was adjusted so that it was midway between the two transducers. When the acoustic wave was applied by the lower transducer, the free surface moved upwards and a hillock appeared above the effective area of the transducer as occurred in the crystal-liquid interface. It eventually stopped moving and fluctuated around an equilibrium height when acoustic radiation pressure and gravity balanced. The reflection coefficient of the acoustic wave at the free surface can be regarded as $R=1$ and thus acoustic radiation pressure is $P=2E$ as is obtained from Eq. (3) given in the discussion section. The balance with the gravity is expressed as

$$\rho_l g\,\delta h = 2E = 2I/c_l. \tag{2}$$

Here, ρ_l, g, δh, E, and I are density of liquid, the gravity acceleration, displacement of the interface, the acoustic energy density and the acoustic power density. The pulse length of the acoustic wave was 5 sec, much longer than that used for the measurement of the crystal-liquid interface in order to see the balance of the forces. It can practically be regarded as a continuous wave. The displacement δh was measured by a high-speed camera. Thus, this power calibration was done under equilibrium conditions and the measurement for the crystal-liquid interface was done under a dynamical condition. Power of the upper transducer was assumed to be the same as the lower one at the same excitation voltage because the coaxes and bonding of the two transducers were exactly the same. We had an uncertainty of ±20% in acoustic wave power by this calibration procedure.

The temperature dependence of h was measured on a rough surface (crystal A, Fig. 3) and a vicinal surface (crystal B, Fig. 4) which were tilted from the c facet by angles of $\theta=43\pm3°$ and $2\pm1°$, respectively. These were determined by the sound velocity or the crystal shape in the growing form. In a lower-temperature region than that shown in these graphs, the displacement was so large and the relaxation was so fast that monitoring the displacement by acoustic wave was not satisfactory. We used the acoustic power density of $I=1.1\times10^2$ W/m^2 for the crystal A and $I=1.5\times10^2$ W/m^2 for the crystal B. The plus sign represents the growth and the minus sign the melting in these figures. Open circles indicate application of the acoustic wave pulse from the crystal side and solid circles application from the liquid side. The displacement h was smaller on the vicinal surface than on the rough surface if we compare them at the same temperature, since the mobility of the vicinal surface was less than the rough surface. The acoustic waves from the liquid side always induced melting in the experimental temperature range on both the rough and the vicinal surfaces. The acoustic waves from the crystal side induced melting in the high temperature range above T_i and the crystallization below T_i for both surface orientations. T_i was lower on the vicinal than the rough surface.

Temperature dependences of h were measured for crystals with different surface orientations in order to investigate the anisotropy of T_i systematically. Orientation dependence of T_i is plotted as circles in Fig. 5. T_i of the rough surfaces in the range of $20°<\theta<50°$ were roughly the same, $T_i=800\pm20$ mK. T_i became anisotropic on the vicinal surface and decreased to 600 mK when approaching the c facet. T_i was reproducible within about 20 mK by changing the power of acoustic waves or by sweeping the temperature.

To investigate the acoustic wave power dependence of h we changed I with the fixed pulse duration of 1 msec. These dependences are plotted above and below T_i for the crystal A in Fig. 6 and the crystal B in Fig. 7. Lines are guides for the eye. They increased linearly for the rough surface. For the vicinal surface we needed a finite power to move the interface. This threshold is probably due to the pinning of steps by the Frank-Read source of the screw dislocations, which is often observed in the growth of the facet. We also measured h by changing the duration of the manipulation pulse with

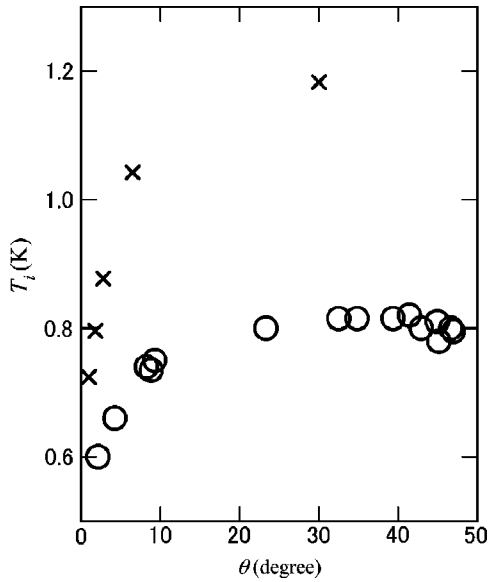

FIG. 5. Surface orientation dependence of inversion temperature T_i plotted as circles. T_i of the rough surfaces in the range of $20° < \theta < 50°$ were roughly the same. T_i were smaller in the vicinal surface and decreased to 600 mK when approaching the *c* facet. Crosses were calculated from Eq. (3) for data taken by Amrit *et al.* in Ref. 12.

$I=150$ W/m^2. This is shown in Fig. 8 for a crystal C with $\theta=4\pm2°$ at $T=500$ mK and h was proportionally increased with the pulse duration. This linearity in power and pulse duration is consistent with the acoustic radiation pressure model shown below.

III. DISCUSSION

When an acoustic wave is applied from medium 1 to medium 2, the acoustic radiation pressure at the interface can be expressed as[20]

$$P = E\left\{1 - \frac{c_1}{c_2} + R^2\left(1 + \frac{c_1}{c_2}\right)\right\}, \tag{3}$$

where

$$E = \frac{\delta P^2}{\rho_1 c_1^2} = \frac{I}{c_1}, \tag{4}$$

δP is the pressure amplitude of the acoustic wave, ρ_1, c_1 are density and sound velocity of media 1, and ρ_2 and c_2 are those of media 2. P is positive when it works in the same direction as the incident wave. R is usually determined by the acoustic impedance of each medium, $z_1=\rho_1 c_1$ and $z_2=\rho_2 c_2$ as

$$R = \frac{z_2 - z_1}{z_1 + z_2}. \tag{5}$$

However, a large value of the growth coefficient $K(T)$ of ^{4}He crystal results in a great enhancement of the acoustic wave reflection. This is because δP induces crystallization and melting at the frequency of acoustic waves at the interface.

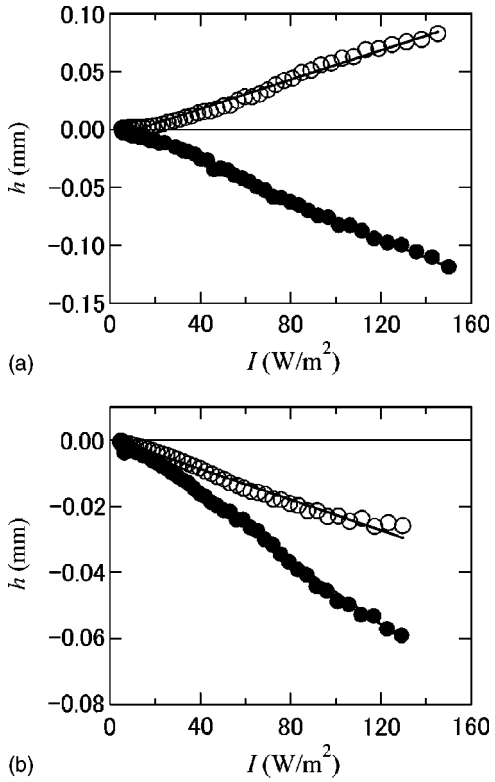

FIG. 6. Acoustic wave power dependence of displacement for a rough surface (crystal A) below [(a) 710 mK] and above [(b) 900 mK] T_i. Open (closed) circles are the case of the acoustic wave from the crystal (liquid) side. Lines are guides for the eye.

The interface becomes a node of the pressure oscillation and pressure fluctuation cannot go through it. The reflection coefficient in the ^{4}He crystal is expressed as[7,9]

$$R(T) = \frac{z_2 - z_1 - z_1 z_2 \rho_1 K(T)\left(\frac{\rho_1 - \rho_2}{\rho_1 \rho_2}\right)^2}{z_1 + z_2 + z_1 z_2 \rho_1 K(T)\left(\frac{\rho_1 - \rho_2}{\rho_1 \rho_2}\right)^2}. \tag{6}$$

$K(T)$ is determined by collisions between an interface and quasiparticles as phonons and rotons, whose densities decrease at low temperatures. This is known to have a functional form of

$$K(T)^{-1} = AT^4 + B\exp\left(\frac{-\Delta}{T}\right). \tag{7}$$

$K(T)$ is very large at low temperature and decreases monotonically on warming. Therefore, $|R(T)|$ decreases from 1 in a low temperature limit to the value determined by Eq. (5) in a high temperature limit, which is small and around 0.2, depending on sound velocity in the crystal.

A negative value of P in Eq. (3) is possible if $|R|$ is small and $c_1 > c_2$. In this case, the radiation pressure works in the direction opposite to the applied direction. This inversion of force has been known at an interface of immiscible fluids such as water and carbon tetrachloride since the 1930's.[28] However, in conventional materials it is not easy to change R

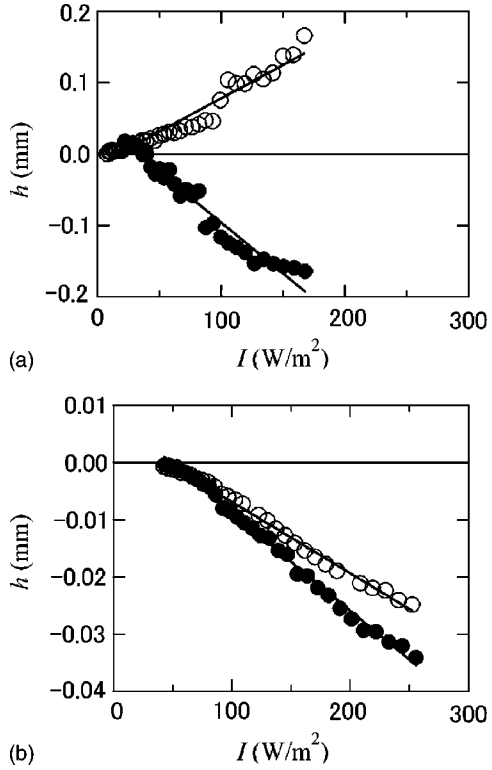

FIG. 7. Acoustic wave power dependence of displacement for a vicinal surface (crystal B) below [(a) 390 mK] and above [(b) 800 mK] T_i. Open (closed) circles are the case of the acoustic wave from the crystal (liquid) side. Small thresholds were needed to move the interface. Lines are guides for the eye.

because R is determined by the acoustic impedance as given by Eq. (5). We can easily control the reflection coefficient continuously and drastically in ^{4}He crystal by changing the temperature as explained above. The velocity of sound in He crystal is always larger than that in the liquid. This means $c_1 > c_2$, when an acoustic wave is applied from the crystal side. Thus inversion of P is realized in ^{4}He above a particular temperature T_i by warming from a low temperature when an acoustic wave is applied from the crystal side. At T_i, the radiation pressure did not impact on the interface because of the balance of reflected and transmitted waves. The vicinal surface has smaller $K(T)$ and $|R(T)|$ than the rough surface if we compare them at the same temperature. Inversion of P should be realized for the vicinal surface at lower temperature than for the rough surface. We can qualitatively explain the orientation dependence of T_i using the concept of acoustic radiation pressure.

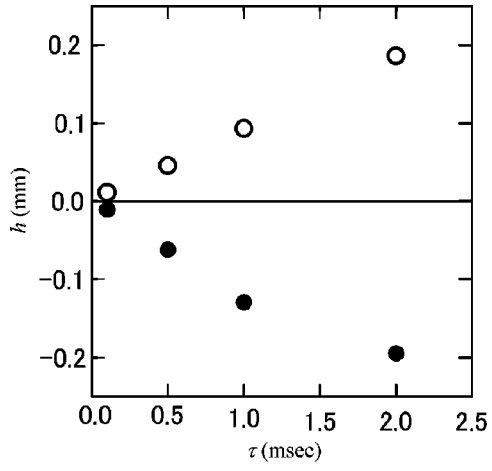

FIG. 8. Pulse duration dependence of the displacement for a crystal C with $\theta = 4°$. Open (closed) circles are the case of the acoustic wave from the crystal (liquid) side. Displacements linearly increased in this range of the pulse width.

In the presence of stress P at the crystal-liquid interface, the driving force for the crystal growth can be written by P/ρ_c using the density of crystal ρ_c.[29,30] Note that acoustic radiation pressure is not a hydrostatic pressure but a stress at the interface. Interface velocity in this driving force is $K(T)P/\rho_c$ and the displacement h by acoustic radiation pressure of duration τ can be written as

$$h = K(T)\frac{P}{\rho_c}\tau. \tag{8}$$

In Eq. (8), the effect of gravity is neglected because h was small in this pulse duration. Dashed and solid lines in Fig. 3 were calculated in this way using $K(T)$ of a rough surface by Bowley and Edwards[31] and by Amrit *et al.*,[12] respectively. The former is a theoretical calculation and the latter is an experiment of acoustic wave reflection. The observed h came between them. The solid lines in Fig. 4 are calculated using $K(T)$ with $\theta = 2.8°$ by Amrit *et al.*[12] We have an error of ±20% in these calculations caused by the uncertainty of the power calibration. We used temperature independent values of I at the interface because damping of the acoustic wave is small and does not make a large difference in these calculations. Agreement with the acoustic radiation pressure model is reasonably good in the low-temperature region and we believe that acoustic radiation pressure does induce the interface motion. Linear dependences of h on τ and I are expected from Eqs. (3), (4), and (8) and are also consistent with the observations in Figs. 6–8. However, we had more melting at high temperatures in both directions of acoustic waves and agreement with acoustic radiation pressure was poor. A simple application of Eq. (3) predicts a higher inversion temperature as shown below. For example, if we set $P = 0$ in Eq. (3) for a crystal with $c_c = 475$ m/sec, $R(T) = 0.36$ is obtained. By comparing this with the reflection coefficient measurement made by Manning *et al.*,[10] who used the same frequency in the same temperature range as ours, we obtain $T_i \approx 1.2$ K, which is significantly higher than our observation.[25] $K(T)$ was measured in several surface orientations by Amrit *et al.* in Ref. 12. We calculated T_i from Eq. (3) in the same way for these orientations and plotted them in Fig. 5 as crosses. They were larger than the observed T_i but had a similar decrease when they got close to the c facet. Growth coefficients of our crystals agreed well with those by Amrit *et al.* as we mentioned, and thus the discrepancy was not caused by the sample quality.

There must be other mechanisms which induce melting at high temperatures. Large anisotropy in T_i indicates that the melting at high temperatures was not caused by a bulk prop-

erty such as mere heating but was a result of the surface effect. Recently Gov proposed that Rychtmyer-Meshikov instability explains the additional melting.[32] This instability model predicts a temperature independent melting and shifts the lines given in Figs. 3 and 4 constant amounts in the negative direction. T_i becomes smaller by this shift and agreement with the experiment is greatly improved. It predicts a different power dependence: $h \propto \sqrt{I}$, which is expected to be recognized as a deviation from the linearity in Figs. 6 and 7. Castaing pointed out the importance of the anharmonicity and the roton contribution on the acoustic radiation pressure.[33] Equation (3) was derived for the interface between two immiscible liquids by neglecting the anharmonicity. This effect may change the form of acoustic radiation pressure of Eq. (3) and also Eq. (2) used for the power calibration. The radiation pressure formula of Eq. (3) may not be applied to the crystal-liquid interface of ^{4}He just as it stands. The crystal-liquid interface is quite different from an ordinary one between immiscible liquids. Radiation pressure is actually a stress and possibly has a component perpendicular to the propagation direction. This component is cancelled in the liquid phase by a movement of liquid out of the acoustic wave beam. In crystal this component induces a transverse strain and may induce additional melting.

Effect of large mobility was taken into account to derive Eq. (6). Even the higher order effect of interface velocity was calculated in Ref. 9, although the effect of acoustic radiation pressure has not yet been considered. Our model is just a combination of Eq. (6) which is well established in ^{4}He and the known formula of acoustic radiation pressure of the ordinary interface, Eq. (3). There is no doubt that acoustic radiation pressure should be considered on a unified basis. We desire a theory that describes a highly mobile interface in an acoustic field taking into account the acoustic radiation pressure.

It was demonstrated systematically that acoustic radiation pressure can be a new driving force for the first order phase transition or crystal growth and melting of ^{4}He in a superfluid. Looking back on the fact that mobility of the interface was determined by collisions with thermal phonons and rotons in ^{4}He, it is not so strange that the interface was moved by applying an acoustic wave or directional phonons. This is a useful tool to manipulate the interface at low temperatures and we will be able to use it to investigate a new type of dynamics in ^{4}He crystal. Will it be possible to induce the crystal growth of other materials such as ice in water by the same method? We will have to use a great deal of acoustic power and wait for a long period to see the effect, because mobility of an interface in ordinary material is minimal compared with a ^{4}He crystal. Application of an acoustic wave with large power and over a long period will cause complicated bulk effects such as a heating of the system and a streaming of the viscous fluid. These effects will disturb the system and make it difficult to extract a pure surface phenomenon such as the acoustic radiation pressure. As explained in the Introduction, ^{4}He crystal in superfluid is an ideal system to avoid these complicated circumstances and to successfully reveal the intrinsic surface effect.

IV. SUMMARY

The crystal-liquid interface motion of ^{4}He induced by acoustic waves was investigated systematically. As reported in our previous paper, the interface moved in the same direction as the acoustic wave at low temperatures and in the opposite direction at high temperatures in the case of an acoustic wave from the crystal side. This means that the direction of force was inverted at T_i. An acoustic wave from the liquid side induced melting only and the direction was the same as the acoustic wave at all experimental temperatures. T_i was measured in crystals with different surface orientations and was about 800 mK for rough surfaces, decreasing to 600 mK on vicinal surfaces when approaching the *c* facet. The temperature dependence of the displacement was compared with an acoustic radiation pressure model and agreement was good in the low-temperature regions. Acoustic wave power and pulse duration dependences were also consistent with this model. Although agreements at low temperatures were reasonably good, additional melting mechanisms are needed to explain the high-temperature behavior, the origin of which we do not know.

ACKNOWLEDGMENTS

We are grateful to M. Uwaha, S. Tamura, and N. Gov for very fruitful discussions and to B. Castaing for useful comments on this experiment. We appreciate T. Tatara and Y. Suzuki for their assistance in this experiment. This study was partly supported by "Ground-based Research Announcement for Space Utilization" promoted by Japan Space Forum, the Sumitomo Foundation and by the Grants-in-Aid for Scientific Research from the Ministry of Education, Culture, Sports, Science and Technology, Japan.

*Electronic address: nomura@ap.titech.ac.jp

[1] A. F. Andreev and A. Y. Parshin, Sov. Phys. JETP **48**, 763 (1978).
[2] S. Balibar and P. Nozières, Solid State Commun. **92**, 19 (1994).
[3] S. G. Lipson and E. Polturak, in *Progress in Low Temperature Physics*, edited by D. F. Brewer (North Holland, Amsterdam, 1987), Vol. XI, p. 127.
[4] K. O. Keshishev, A. Y. Parshin, and A. V. Babkin, JETP Lett. **31**, 724 (1980).
[5] C. L. Wang and G. Agnolet, Phys. Rev. Lett. **69**, 2102 (1992).
[6] E. Rolley, C. Guthmann, E. Chevalier, and S. Balibar, J. Low Temp. Phys. **99**, 851 (1995).
[7] B. Castaing and P. Nozières, J. Phys. (France) **41**, 701 (1980).
[8] B. Castaing, S. Balibar, and C. Laroche, J. Phys. (France) **41**, 897 (1980).
[9] M. Uwaha and P. Nozières, J. Phys. (France) **46**, 109 (1985).
[10] M. B. Manning, M. J. Moelter, and C. Elbaum, J. Low Temp. Phys. **61**, 447 (1985).

[11] M. J. Graf and H. J. Maris, Phys. Rev. B **35**, 3142 (1987).
[12] J. Amrit, P. Legros, and J. Poitrenaud, J. Low Temp. Phys. **100**, 121 (1995).
[13] M. A. Grinfeld, Sov. Phys. Dokl. **31**, 831 (1986).
[14] R. H. Torii and S. Balibar, J. Low Temp. Phys. **89**, 391 (1992).
[15] P. E. Wolf, D. O. Edwards, and S. Balibar, J. Low Temp. Phys. **51**, 489 (1983).
[16] P. Nozières and M. Uwaha, J. Phys. (France) **47**, 263 (1986).
[17] L. A. Maksimov and V. L. Tsymbalenko, JETP **95**, 455 (2002).
[18] L. Rayleigh, Philos. Mag. **3**, 338 (1902).
[19] L. Brillouin, Ann. Phys. (Leipzig) **4**, 528 (1925).
[20] F. E. Borgnis, Rev. Mod. Phys. **25**, 653 (1953).
[21] M. Sato and T. Fujii, Phys. Rev. E **64**, 026311 (2001).
[22] T. G. Wang, E. H. Trinh, A. P. Croonquist, and D. D. Elleman, Phys. Rev. Lett. **56**, 452 (1986).
[23] R. E. Apfell, Y. Tian, J. Jankovsky, T. Shi, X. Chen, R. G. Holt, E. Trinh, A. Croonquist, K. C. Thornton, A. Sacco, Jr., C. Coleman, F. W. Leslie, and D. H. Matthiesen, Phys. Rev. Lett. **78**, 1912 (1997).
[24] M. J. Marr-Lyon, D. B. Thiessen, and P. L. Marston, Phys. Rev. Lett. **86**, 2293 (2001).
[25] R. Nomura, Y. Suzuki, S. Kimura, and Y. Okuda, Phys. Rev. Lett. **90**, 075301 (2003).
[26] R. Nomura, Y. Suzuki, S. Kimura, Y. Okuda, and S. Burmistrov, Fiz. Nizk. Temp. **29**, 663 (2003) [Low Temp. Phys. **29**, 492 (2003)].
[27] R. H. Crepeau, O. Heybey, D. M. Lee, and S. A. Strauss, Phys. Rev. A **3**, 1162 (1971).
[28] G. Hertz and H. Mende, Z. Phys. **114**, 354 (1939).
[29] S. Balibar, D. O. Edwards, and W. F. Saam, J. Low Temp. Phys. **82**, 119 (1991).
[30] J. Bodensohn, K. Nicolai, and P. Leiderer, Z. Phys. B: Condens. Matter **64**, 55 (1986).
[31] R. M. Bowley and D. O Edwards, J. Phys. (France) **44**, 723 (1983).
[32] N. Gov, cond-mat/0302183.
[33] B. Castaing (private communication).